Neurochemical Research (2019) 44:1690–1702
https://doi.org/10.1007/s11064-019-02797-2

ORIGINAL PAPER

Inhibition of MicroRNA-195 Alleviates Neuropathic Pain by Targeting Patched1 and Inhibiting SHH Signaling Pathway Activation

Xuhui Wang[1] · Hong Wang[1] · Tao Zhang[3] · Meng He[2] · Hong Liang[1] · Hao Wang[1] · Lunshan Xu[1] · Sha Chen[2] · Minhui Xu[1]

Received: 10 December 2018 / Revised: 11 March 2019 / Accepted: 10 April 2019 / Published online: 19 April 2019

Abstract
Trigeminal neuralgia (TN) is a type of chronic neuropathic pain that is caused by peripheral nerve lesions that result from various conditions, including the compression of vessels, tumors and viral infections. MicroRNAs (miRs) are increasingly recognized as potential regulators of neuropathic pain. Previous evidence has demonstrated that miR-195 is involved in neuropathic pain, but the mechanism remains unclear. To investigate the pathophysiological role of miR-195 and Shh signaling in TN, persistent facial pain was induced by infraorbital nerve chronic constriction injury (CCI-IoN), and facial pain responses were evaluated by Von Frey hairs. qPCR and Western blotting were used to determine the relative expression of miR-195 and Patched1, the major receptor of the Sonic Hedgehog (Shh) signaling pathway, in the caudal brain stem at distinct time points after CCI-IoN. Here, we found that the expression of miR-195 was increased in a rat model of CCI-IoN. In contrast, the expression of Patched1 decreased significantly. Luciferase assays confirmed the binding of miR-195 to Patched1. In addition, the overexpression of miR-195 by an intracerebroventricular (i.c.v) administration of LV-miR-195 aggravated facial pain development, and this was reversed by upregulating the expression of Patched1. These results suggest that miR-195 is involved in the development of TN by targeting Patched1 in the Shh signaling pathway, thus regulating extracellular glutamate.

Keywords MicroRNA-195 · Neuropathic pain · Patched1 · Sonic Hedgehog

Introduction

TN is a type of severe and paroxysmal facial pain and has a strong negative impact on quality of life. Although most primary TN patients can be cured with microvascular decompression (MVD) [1], for TN patients who are not suited for open Surgery or show no response to MVD, there is no effective treatment.

Refractory and chronic neuropathic pain commonly results from injuries or diseases of peripheral nerves and the consequent sensitization of central nociceptive pathways [2]. However, the exact pathophysiological mechanisms remain unknown. Gene expression and regulation is an essential mechanism in neuropathic pain. Recent studies suggest that the expression of various microRNAs, including miR-183, miR-195, miR-124, and miR-125 are induced in neuropathic pain [3, 4]. Some targets of these microRNAs have been identified, including Nav1.3, BDNF, Cav1.2, and Scn2b, respectively [4], the auxiliary voltage-gated calcium channel subunits α2δ-1 and α2δ-2 and a special, light-touch-sensitive neuronal type that normally does not elicit pain but is recruited during mechanical allodynia [5]. A recent study reported that miR-195 levels are associated with neuropathic pain in rats [6]. However, the mechanism remains unclear.

✉ Sha Chen
925896877@qq.com

✉ Minhui Xu
minhuixu66@aliyun.com

[1] Department of Neurosurgery, Research Institute of Surgery Daping Hospital, Third Military Medical University (Army Medical University), No. 10 Changjiangzhilu Rd, Yuzhong District, Chongqing 400042, People's Republic of China

[2] Department of Clinical Biochemistry, Laboratory Sciences, Third Military Medical University (Army Medical University), No. 30 Gaotanyan Street, Shapingba District, Chongqing 400038, People's Republic of China

[3] Department of Neurology, The 303rd Hospital of PLA, Nanning, No. 52 Zhiwu Street, Qingxiu District, Nanning 530021, People's Republic of China

Previous evidence has shown that the Shh family plays an important role in brain development, stem cell biology, tissue homeostasis and cancers [7, 8], maintains many adult nerve structures and regulates the proliferation of various progenitor cells [9]. Recently, some evidence has shown that Shh might protect some neural tissues against injuries and induce the compensatory proliferation of neural tissues post-traumatically [10, 11]. Peripheral nerve tissue injury is an important cause of neuropathic pain, and it is sensible to deduce that Shh is involved in neuropathic pain. A few studies have demonstrated that Shh signaling is required for nociceptive sensitization in neuropathic pain in rats [12, 13]. However, its up- and downstream mechanisms are not yet completely clear.

Herein, we show that Patched1, an inhibitory receptor of the Shh signaling pathway, is the direct target of miR-195. Moreover, we report that miR-195 is involved in neuropathic pain by activating Shh signaling.

Materials and Methods

Ethics Statement

This study was carried out in strict accordance with the recommendations in the Guide for the Care and Use of Laboratory Animals of the Third Military Medical University (Army Medical University). All procedures were performed according to protocols approved by the ethics committee of the Third Military Medical University, and adult male Sprague–Dawley rats were purchased from its Experimental Animal Center. The ethical permit number is SCXK2014-0004.

Animals and Trigeminal Neuralgia Model

The study was approved by the Committee for the Protection of Animal Care Committee at the Third Military Medical University. Adult male Sprague–Dawley rats weighing between 210 and 245 g were housed 3–4 per cage in a temperature-control environment with a 12/12-h light–dark cycle. Water and food were available ad libitum. Chronic constriction injury of the infraorbital nerve (CCI-IoN) was performed following the procedures established by Vos et al. [14] and Dieb et al. [15]. Briefly, rats were anesthetized by an intraperitoneal (i.p.) injection of pentobarbital (65 mg/kg) and fixed to a board. All surgeries were performed under the direct visual control of a microscope (6×). A 1-cm-long incision was made in the gingivobuccal margin, and the IoN was dissected free. Two ligatures (using 5–0 chromic gut sutures), separated by 1–2 mm, were loosely tied around the IoN, reducing the diameter of the IoN slightly without blocking the superficial vasculature to the nerves. The incision was sutured with 5–0 silk sutures. For the sham group animals, the IoN was isolated without ligation. The operation was conducted in a temperature-controlled environment ($22 \pm 1^{\circ}$ C), and a cotton blanket was used to maintain the animal's body temperature.

Behavioral Test and Analysis

According to the procedures used in previous studies by Vos et al. [14] and Han et al. [16], mechanical allodynia was induced with a graded series of Von Frey hairs, consisting of 1 g, 2 g, 4 g, 9 g and 16 g, and assessed by a second experimenter according to the method used by Vos et al. The rats' responses to mechanical stimulation consisted of one or more of the following elements: detection, withdrawal, escape/attack, and asymmetric grooming. Each category was given a score (0–4) based on the number of observed response elements (Table 1).

Intracerebroventricular (i.c.v.) Catheter Insertion and the Measurement of Glutamate in the Cerebrospinal Fluid (CSF)

Each rat was anesthetized via an intraperitoneal injection of chloral hydrate (300 mg/kg). The head was fixed on a stereotaxic frame under sterile conditions, and a 21-gauge stainless-steel guide cannula (12 mm) was implanted in the right lateral ventricle. The stereotaxic coordinates were 0.8 mm posterior, 1.5 mm right lateral, and 4.0 mm ventral to bregma, according to Paxinos and Watson [17]. The guide cannula was fixed to two stainless screws

Table 1 Response scoring system

Response category	Observed response elements				
	Detection	With-drawal	Escape/attack	Face-grooming	Score
No response	0	0	0	0	0
Non aversive response	1	0	0	0	1
Mild aversive response	1	1	0	0	2
Strong aversive response	1	1	1	0	3
Prolonged aversive behavior	1	1	1	1	4

anchored to the skull with bone cement and sealed with a cannula rod. Motor deficiencies and signs of infection were monitored after surgery, and rats with any deficits were excluded from further experimentation. The rats were allowed to recover for 7 days and then used for subsequent experiments [18]. The lentivirus-miR-195 mimic, lentivirus-miR-195 inhibitor, lentivirus-Patched1, and lentivirus-shPatched1 were purchased from Genepharma (Shanghai, China). Ten microliters of recombinant lentivirus (10^7 p.f.u. viruses per rat) was delivered by i.c.v. administration every other day from days 0 to 6 after CCI using a microinjection syringe through a PE-20 catheter filled with drug and connected to the guide cannula.

Throughout the experiment, CSF was collected from rats anesthetized by chloral hydrate. The animals were placed in a prone position with the neck flexed. The occipital muscles of the rats were separated, and the atlantooccipital membrane was exposed. We punctured the cisterna magna and extracted 100–200 µl of CSF [19]. After centrifugation at 250×*g*, 10 min, we removed the supernatant and froze it at − 80 °C. Glutamate was measured using high-performance liquid chromatography (HPLC). The analysis was carried out by using a Waters HPLC system (Waters Breeze 1525, Etten-Leur, Netherlands) equipped with an isocratic pump (Waters 1515), an autosampler (Waters 2707) and a UV–Visible detector (Waters 2489). Then, the caudal medulla was removed and frozen for analysis.

Western Blotting

Total protein from the tissues was prepared after treatment with RIPA buffer (Beyotime, Shanghai, China). The BCA protein assay was used to determine protein concentrations. For the Western blot assay, proteins (50 µg/well) were separated by 8% sodium dodecylsulfate polyacrylamide gel electrophoresis (SDS-PAGE) and then transferred to a polyvinylidene difluoride (PVDF) membrane (Millipore, Billerica, MA, USA). After blocking with 5% nonfat milk for 2 h at room temperature, the membranes were incubated overnight at 4 °C with specific primary antibodies. The following antibodies were used: mouse anti-Patched1 (1:800; Novus Biologicals, Littleton, USA), anti-Gli2 (1:1000; Proteintech Rosemont, USA), anti-SUFU (1:1000; Cell Signaling Technology, USA) and mouse anti-β-actin (1:5000; Cell Signaling Technology, USA). The blots were then washed in TBST (Tris-buffered saline (TBS) containing 0.1% Tween 20) and incubated in the appropriate secondary antibody for 1 h at room temperature. Immunoreactive bands were detected with an ECL kit (Millipore, Billerica, MA, USA) according to the manufacturer's instructions.

Quantitative Real-Time RT-PCR Analysis

Total RNA was extracted from the tissues using Trizol reagent (Invitrogen, Carlsbad, CA, USA) according to the manufacturer's instructions. The amount of RNA was measured using a spectrophotometer. The reverse transcription reactions were performed using the M-MLV Reverse Transcriptase kit (Invitrogen) and the PrimeScript® miRNA cDNA Synthesis kit (Perfect Real Time; TaKaRa, Dalian, China). The Thermo Scientific Maxima SYBR Green qPCR Master Mix kit (Thermo Scientific) was used to detect the expression of miR-195 and the mRNA expression of Patched1. U6 snRNA and GAPDH were used as internal controls for the expression of miRNA and mRNA, respectively. Each sample was analyzed in triplicate. The $2^{-\Delta\Delta Ct}$ method was used to quantify the relative levels of gene expression.

Luciferase Reporter Assay

The 3′-UTR of Patched1 harboring either the seed sequence of the miR-195 wild-type binding sites or the mutant binding sites was cloned into the pmirGLO dual-luciferase vector (Promega, Madison, WI, USA). For the luciferase assay in 293T cells, cells seeded at a density of 1.0×10^6 cells per well in 24-well plates were cotransfected with the Luc-pGL3-Patched1-WT-3′UTR or Luc-pGL3-Patched1-MUT-3′UTR vector and miR-195 mimic or scrambled miRNA using Lipofectamine 2000 (Invitrogen, Carlsbad, CA, USA) following the manufacturer's instructions. After transfection for 48 h, the cells were harvested for detection using a dual-luciferase reporter assay kit (Promega, Madison, WI, USA). The results are expressed as the relative luciferase activity (firefly Luc/renilla Luc). All experiments were repeated three times.

Cell Culture

293T cells were purchased from the Cell Bank of the Committee on Type Culture Collection of the Chinese Academy of Sciences (CCTCC, Shanghai, China). Cells were cultured in Dulbecco's modified Eagle's medium (DMEM, Gibco, Carlsbad, CA, USA) supplemented with 10% fetal bovine serum (FBS), 100 U/ml penicillin and 0.1 mg/ml streptomycin. Antibiotics and FBS were purchased from HyClone (Waltham, MA, USA). The cells were maintained under an atmosphere of 95% air and 5% CO_2 at 37 °C.

Statistical Analysis

Data are reported as the mean and standard error of the mean (SEM) from at least three independent experiments, and the *P* value was evaluated and calculated using a two-tailed

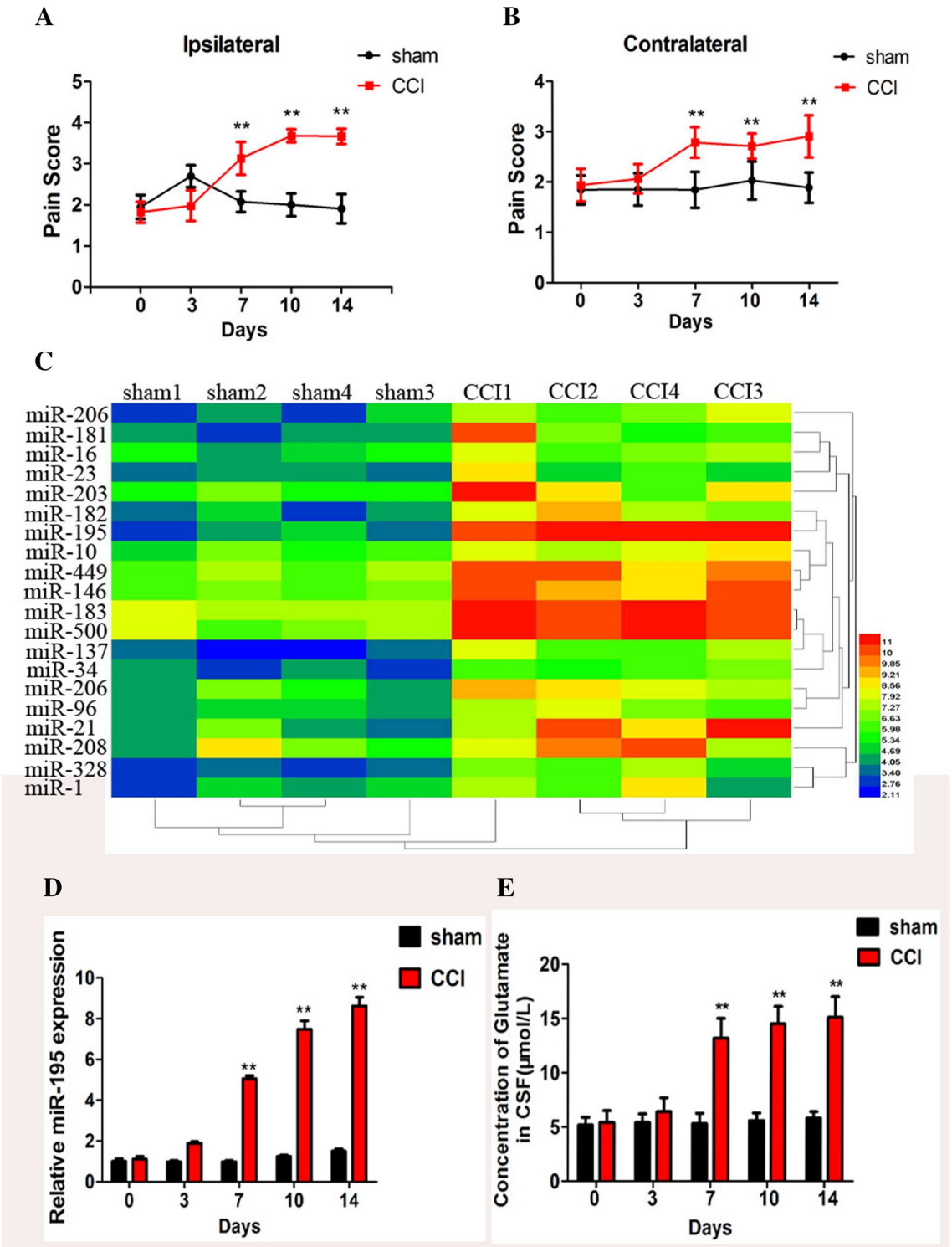

paired *t* test. When there were multiple factors involved, a two-way analysis of variance (ANOVA) was used; multiple groups were compared using a one-way or two-way ANOVA. Values of $P < 0.05$(*) were considered statistically significant. Values of $P < 0.01$(**) were considered statistically significant.

Results

Expression Levels of miR-195 Are Increased in a Rat Model of CCI-IoN

A decline was shown in mechanical allodynia within 7 days

◂**Fig. 1** The expression of miR-195 is increased in a rat model of CCI-IoN. **a, b** The effect on CCI-induced neuropathic pain (ipsilateral and contralateral) was determined on days 0, 3, 7, 10 and 14 post-CCI-IoN. Each bar represents the mean ± S.D., N = 6 for each time point, $^{**}p < 0.01$ versus sham group. **c** A heatmap of negative delta cycle threshold values showing changes in miRNA expression in the caudal medulla of rats that underwent CCI-IoN surgery on postoperative day 7. Each row represents a miRNA, and each column represents a caudal medulla sample. Red represents high expression, and blue represents low expression. Based on the results of a t-test, volcano plot filtering was performed between the two groups. Twenty significant miRNAs were upregulated in the CCI-IoN model rats compared with the control rats. $p < 0.01$ was used (N = 5 per group). **d** The expression of miR-195 in the caudal medulla of rats that underwent CCI-IoN surgery was examined by RT-PCR on days 0, 3, 7, 10 and 14 after CCI-IoN. $^{**}p < 0.01$ compared with the sham group. **e** The concentration of glutamate was measured in the cerebrospinal fluid (CSF) of the rat model on days 0, 3, 7, 10 and 14 post-CCI-IoN. $^{**}p < 0.01$ versus sham (Color figure online)

after surgery both on the ipsilateral side and on the contralateral side in the rat CCI-IoN model, and this decline lasted for 14 days after surgery (Fig. 1a, b). Glutamate levels are related to neuropathic pain. Here, we found that the glutamate level in the cerebrospinal fluid (CSF) was markedly increased in the CCI-IoN group compared to the sham group at postoperative day 7, and this increase lasted for 14 days (Fig. 1e). These results indicated that the nerve injury model was successful in establishing mechanical allodynia. Microarray analysis of small RNAs was also performed. Using a paired t-test, 20 miRNAs were found to be differentially expressed between the CCI group and the sham group ($P < 0.01$, false discovery rate < 0.05; Fig. 1c).

Among these miRNAs, miR-195 was one of the most prominently upregulated miRNAs (Fig. 1c). We also found that miR-195 expression was significantly increased on postoperative days 0, 3, 7, 10 and 14 (Fig. 1d) in CCI-IoN rats compared to rats that received sham surgery, and the concentration of glutamate was also significantly increased on postoperative days 7, 10 and 14 (Fig. 1e), implying a positive correlation between miR-195 expression and TN development in CCI-IoN rats.

Overexpression of miR-195 Aggravates Neuropathic Pain Development

To investigate the biological effect of miR-195 in TN, we experimentally overexpressed miR-195 expression in rats by an intracerebroventricular injection of lentivirus carrying miR-195 (LV-miR-195). The expression of miR-195 was significantly increased in CCI-IoN rats infected with LV-miR-195 (Fig. 2a). We also tested the CSF and found that the glutamate level in the CSF was markedly increased by miR-195 overexpression on postoperative days 0, 3, 7, 10 and 14 (Fig. 2b). Interestingly, subsequent behavior experiments showed that ipsilateral mechanical allodynia was significantly aggravated by miR-195 overexpression only on postoperative day 7, but on the contralateral side, this significant difference in mechanical allodynia was observed from postoperative day 7 on (Fig. 2c–d). These results indicate a facilitative role for miR-195 in TN.

Patched1, an Inhibitory Receptor of the SHH Signaling Pathway, Is Downregulated in Response to TN Development

We measured the expression of Patched1, an inhibitory receptor of the SHH signaling pathway in the caudal medulla of CCI-IoN rats via quantitative real-time PCR analysis and Western blot analysis. In our study, we found that the mRNA and protein expression levels of Patched1 were significantly decreased in the caudal medulla of the CCI-IoN group on postoperative days 3, 7, 10 and 14 compared with those in the same region of the sham group (Fig. 3a–c). This result contradicts our previous study on miR-195 expression.

Patched1 Is a Direct Target of miR-195

To predict whether the 3′-UTR of Patched1 mRNA contains a miR-195 binding site, TargetScan 7.1 was used. Our results indicate that the seed sequence of miR-195 is paired with the Patched1 3′-UTR in both humans and rats (Fig. 4a). To verify whether miR-195 targets the Patched1 3′-UTR, a dual luciferase reporter vector containing the sequence of the Patched1 3′-UTR was designed (pmirGLO Patched1 3′-UTR, WT-Patched1). 293T cells were cotransfected with the wild-type plasmid vector and three different doses (10, 50, and 100 nM) of miR-195 mimics. The miR-195 mimics reduced the relative luciferase activity in a dose-dependent manner (Fig. 4b). We also inserted the Patched1 3′-UTR harboring a mutant binding site (MUT-Patched1) into the dual-luciferase vector (Fig. 4c). Cotransfection of miR-195 mimics with the luciferase vector containing WT-Patched1 resulted in a significant decrease in relative luciferase activity compared with that of the scrambled miRNA (Fig. 4d). However, mutated binding sites abrogated the inhibitory effect of miR-195 overexpression on relative luciferase activity (Fig. 4d), implying that miR-195 directly targets the 3′UTR of Patched1 mRNA. Furthermore, the overexpression of miR-195 mimics (50 and 100 nM) significantly inhibited Patched1 mRNA and protein levels compared with those in cells transfected with scramble miRNA in a dose-dependent manner (Fig. 4e–g). These findings suggest that the Patched1 gene is a direct target of miR-195 and that miR-195 inhibits the expression of Patched1.

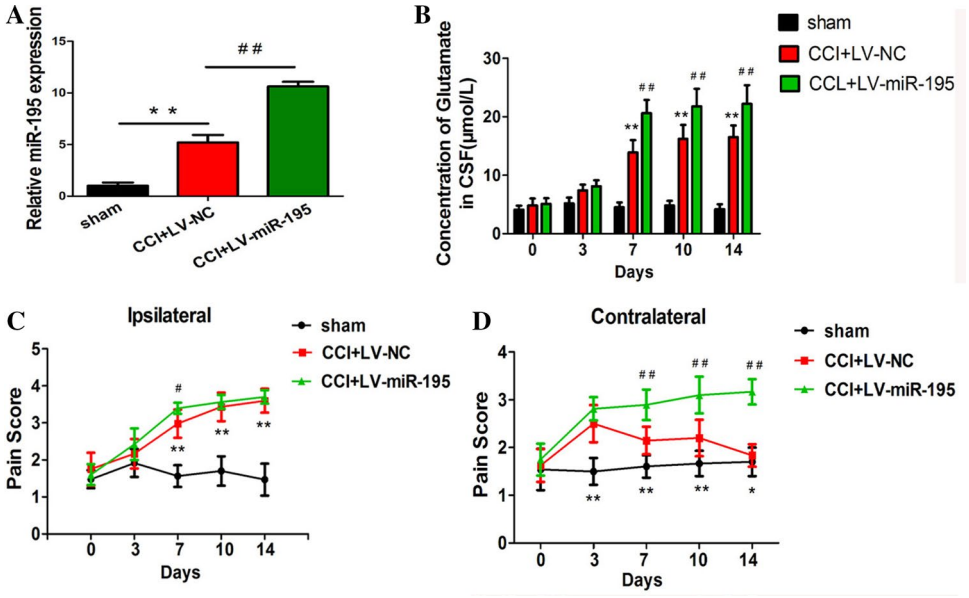

Fig. 2 Overexpression of miR-195 aggravates neuropathic pain development. **a** The expression of miR-195 in CCI-IoN rats infected with LV-miR-195 or LV-negative control (NC) by RT-PCR on post-operative day 7. $^{**}p<0.01$ versus sham group; $^{\#\#}p<0.01$ versus CCI + LV − NC. **b** The concentration of glutamate was measured in the cerebrospinal fluid (CSF) of CCI-IoN rats infected with LV-miR-195 or LV-negative control (NC) on days 0, 3, 7, 10 and 14. $^{*}p<0.01$ versus sham group; $^{\#\#}p<0.01$ versus CCI + LV − NC. **c**, **d** The effect of miR-195 overexpression on neuropathic pain was assessed by the analysis of behavioral tests. $^{**}p<0.01$ versus sham group; $^{\#\#}p<0.01$, $^{\#}p<0.05$ versus CCI + LV − NC; N = 6 for each group

Patched1 Is Responsible for miR-195-Mediated Neuropathic Pain

To investigate whether miR-195 exerts its function in regulating facial neuropathic pain by targeting Patched1, we performed experiments in which rats were infected with LV-miR-195, LV-miR-195 inhibitor, LV-Patched1, or LV-sh Patched1, or coinfected with LV-miR-195 and LV-Patched1 or LV-miR-195 inhibitor and LV-sh Patched1 after CCI-IoN. The results showed that the miR-195 inhibitor markedly decreased facial pain in CCI-IoN rats compared with control rats (Fig. 5a). Moreover, facial pain was also attenuated when we infected the rats with LV-Patched1 (Fig. 5a). Conversely, similar to the results in CCI-IoN rats infected with LV-miR-195, facial pain was significantly aggravated when we infected the rats with LV-sh Patched1, but this was mainly observed on the contralateral side (Fig. 5a). Meanwhile, the facilitated effects of miR-195 overexpression on neuropathic pain were also markedly reversed by Patched1 overexpression when we coinfected the rats with LV-miR-195 and LV-Patched1 (Fig. 5a). However, knockdown of Patched1 blocked the inhibitory effect of the miR-195 inhibitor on TN when we coinfected the rats with LV-miR-195 inhibitor and LV-sh Patched1 (Fig. 5a).

To determine the expression of miR-195 and Patched1 in the caudal medulla of CCI-IoN rats, we performed qRT-PCR and Western blot analyses (on tissues acquired on day 7 post-CCI-IoN surgery). The results also showed that the overexpression of miR-195 mimics in the rats resulting from an intracerebroventricular injection of LV-miR-195 markedly suppressed Patched1 mRNA and protein expression, and these levels were significantly increased by an intracerebroventricular injection of LV-miR-195 inhibitor (Fig. 5b–d). The decreased expression of Patched1 induced by miR-195 overexpression was also reversed by Patched1 overexpression when we coinfected the rats with LV-miR-195 and LV-Patched1 (Fig. 5b–d). The knockdown of Patched1 significantly reversed the promoting effect of the miR-195 inhibitor on Patched1 expression when we coinfected the rats with LV-miR-195 inhibitor and LV-sh Patched1 (Fig. 5b–d). Taken together, these results indicate that miR-195 promotes neuropathic pain by targeting Patched1.

miR-195 Increases the Extracellular Glutamate Levels and Is Involved in TN Through the SHH Signaling Pathway

To further investigate the underlying molecular mechanism of the role of miR-195 in regulating neuropathic pain, the protein expression of SUFU (an inhibitory regulation factor of the Shh signaling pathway) and Gli2 (a positive regulation factor of the Shh signaling pathway) was measured. In line with Patched1 expression, compared to the sham groups,

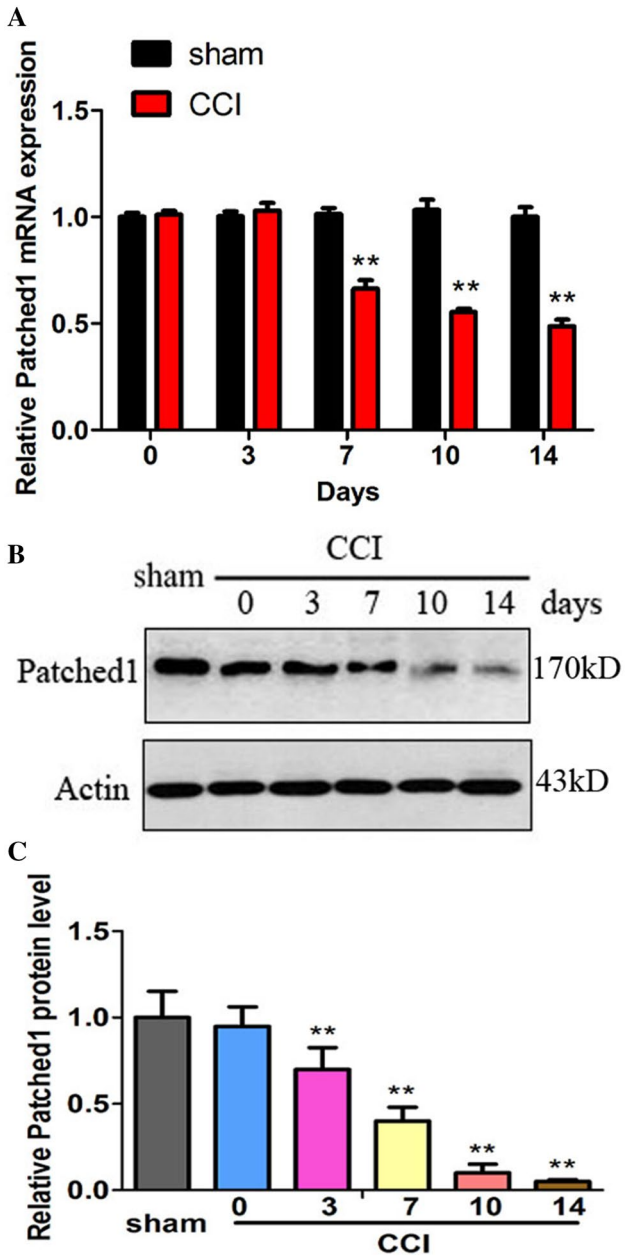

Fig. 3 Patched1 is downregulated in response to TN development. **a** The expression of Patched1 in the caudal medulla of the rats was examined by RT-PCR on days 0, 3, 7, 10 and 14 after CCI-IoN. $^{**}p < 0.01$ compared with the sham group. N = 6 for each group **b** The protein expression level of Patched1 in the caudal medulla of the rats was tested by Western blotting on days 0, 3, 7, 10 and 14 after CCI-IoN. **c** Patched1 protein expression was quantified using Quantity One software after normalization with Actin. $^{**}p < 0.01$ versus sham. N = 3 for each group in **b** and **c**

the CCI-IoN group exhibited significantly decreased SUFU expression and increased Gli2 expression in the caudal medulla at the level of both mRNA and protein (Fig. 6a–e). In addition, the overexpression of miR-195 markedly increased Gli2 expression but repressed SUFU expression in CCI-IoN rats. These results were reversed by infection with LV-miR-195 inhibitor (Fig. 6a–e). An intracerebroventricular injection of LV-Patched1 resulted in elevated SUFU expression and decreased GLI2 expression on day 7 postinjection. The effect of an intracerebroventricular injection of LV-sh Patched1 was the opposite (Fig. 6a–e). The increased expression of Gli2 and the decreased expression of SUFU induced by miR-195 overexpression were also reversed by Patched1 overexpression when we coinfected the rats with LV-miR-195 and LV-Patched1 (Fig. 6a–e). Furthermore, the knockdown of Patched1 significantly reversed the effect of the miR-195 inhibitor on SUFU and Gli2 expression when we coinfected the rats with LV-miR-195 inhibitor and LV-sh Patched1 in TN rats (Fig. 6a–e). These results show that the regulation of Patched1 alters the effect of miR-195 and the miR-195 inhibitor on neuropathic pain development and the Shh signaling pathway, indicating that miR-195 functions by targeting Patched1 and regulating the Shh signaling pathway.

Collectively, our results show that miR-195 exerts its promoting effect on TN development by targeting Patched1. Shh signaling participates in epilepsy development by regulating extracellular glutamate levels [20], an important factor related to neuropathic pain [19, 21]. To explore the mechanism by which miR-195 regulates neuropathic pain, we assessed glutamate concentrations in the cerebrospinal fluid (CSF) and found that the glutamate levels in the CSF markedly increased in the CCI-IoN group compared with the sham group (Fig. 6f). The glutamate levels were significantly increased in CCI-IoN rats infected with LV-miR-195 and markedly decreased in rats infected with the miR-195 inhibitor (Fig. 6f). The administration of LV-Patched1 and LV-sh Patched1 decreased the glutamate levels in the CSF and influenced facial pain (Fig. 6f). The increased level of glutamate induced by miR-195 overexpression was also reversed by Patched1 overexpression when we coinfected the rats with LV-miR-195 and LV-Patched1 (Fig. 6f). The knockdown of Patched1 significantly reversed the inhibitory effect of the miR-195 inhibitor on glutamate levels when we coinfected the rats with LV-miR-195 inhibitor and LV-sh Patched1 (Fig. 6f). This evidence reveals that miR-195 and Patched1 are crucial players in neuropathic pain.

Discussion

Our results show that miR-195 aggravates mechanical allodynia in CCI rats by upregulating the Shh signaling pathway. miR-195 is upregulated due to the CCI-IoN procedure, and it targets Patched1, an inhibitory receptor of the Shh signaling pathway, and reduces its expression, resulting in the activation of the Shh signaling pathway (as evidenced by the increased expression of Gli2 and the decreased expression of SUFU). These effects also aggravate facial pain by elevating

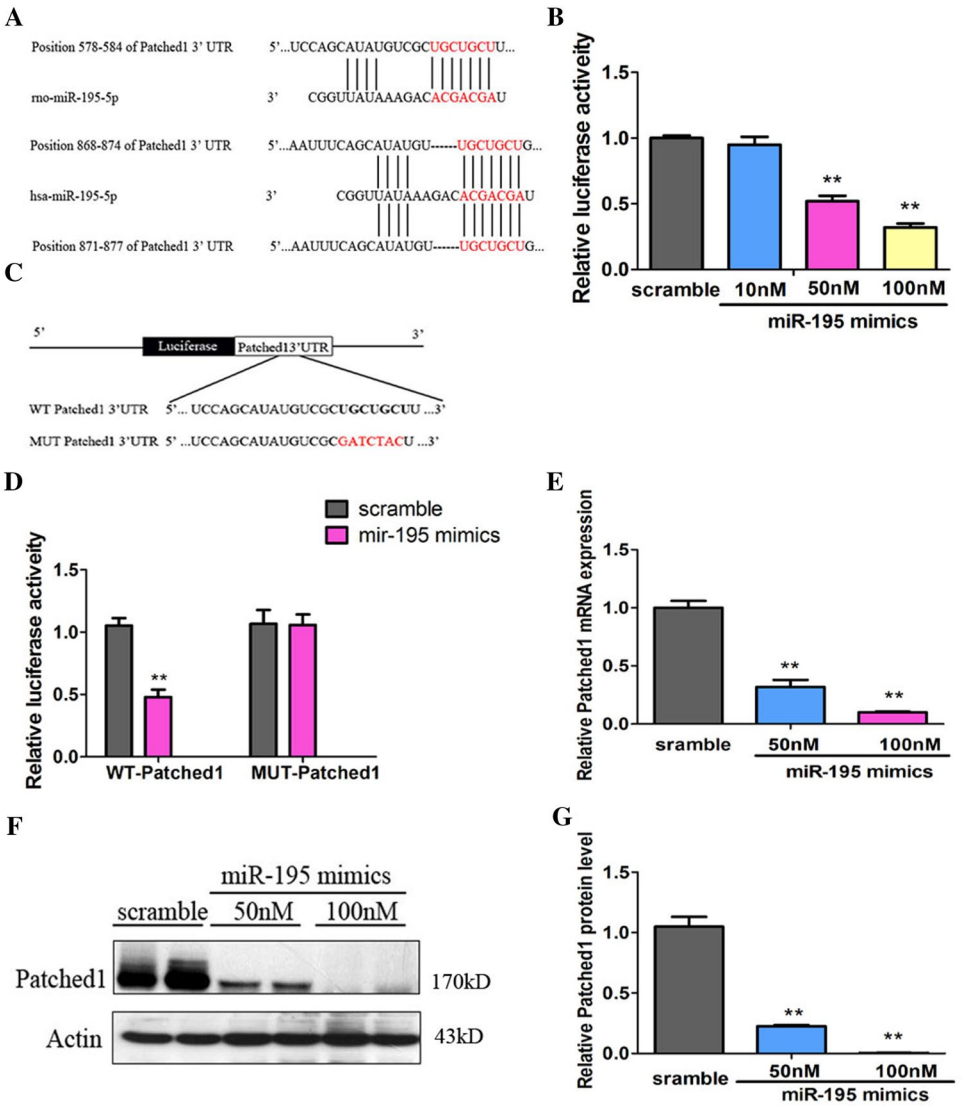

Fig. 4 Patched1 is a direct target of miR-195. **a** The matched seed region between miR-195 and the Patched1 3′UTR predicted by target scan is in red. **b** miR-195 mimics decreased the relative luciferase activity in a dose-dependent manner when cotransfected with wild-type (WT) Patched1 3′UTR plasmid vector in 293T cells. $^{**}p < 0.01$ versus scramble. One-way ANOVA, N = 3. **c** miR-195 targets wild-type Patched1 3′-UTR, but not its mutant. Luciferase constructs bearing a Patched1 3′-UTR (WT) or Patched1 3′-UTR containing mutated binding sequences of miR-195 (Mut) were cotransfected with miR-195. **d** Dual-luciferase reporter assay of miR-195 and Patched1 3′-UTR. 293T cells were cotransfected with miR-195 mimics and the dual-luciferase vector containing WT-Patched1 or MUT-Patched1 and incubated for 48 h. The relative luciferase activity was measured using the Dual-Luciferase Assay System. $^{*}p < 0.05$, $^{**}p < 0.01$ versus scramble. **e** The relative expression of Patched1 mRNA and protein **f**, **g** 293T cells treated with miR-195 mimics in a dose-dependent manner compared with the scramble group. $^{**}p < 0.01$ versus scramble. N = 3 for each group in **b**, **d**, **e**, **f** and **g** (Color figure online)

the concentration of extracellular glutamate (Fig. 7). These findings add to the growing evidence for the crucial role of miR-195 in the regulation of neuropathic pain and may help establish miR-195 as a biomarker or therapeutic target for TN and other types of orofacial neuropathic pain in the future.

In this study, our results initially showed that the expression of miR-195 gradually and markedly increased in the caudal medulla after CCI-IoN surgery. We administered LV-miR-195 via an intracerebroventricular catheter, resulting in the upregulated expression of miR-195. After that, significantly worse allodynia was observed bilaterally. In fact, exacerbated allodynia was easily observed on the contralateral side. We hypothesized that the odd results could likely be ascribed to the limitations of the methods of the pain test. In a previous study by Vos et al. [14], four responses to mechanical stimulation for each rat were used to assess the degree of facial pain degree so that the highest possible score was only 4. If the degree of facial pain was beyond this range, this method would be unable to assess the degree of pain accurately. According to our results, the mean pain score was approximately 3.5 on day 10 after surgery. In this situation, even though the actual degree of pain obviously increased due to the upregulated expression of miR-195, it was difficult to observe the significant differences between these two groups. In contrast, the contralateral pain score was significantly lower than the ipsilateral score postoperatively, so the increase in the degree of facial pain was more noticeable. The results showed that infection with LV-miR-195 inhibitor obviously alleviated facial pain in the TN rats, suggesting that miR-195 participates in and promotes TN development. Similar to our results, Shi et al. found that upregulated miR-195 in spinal microglia of rats with SNL contributes to neuropathic pain by inhibiting autophagy and inducing neuroinflammation [6]. However, they did not detect the expression of miR-195 in neurons

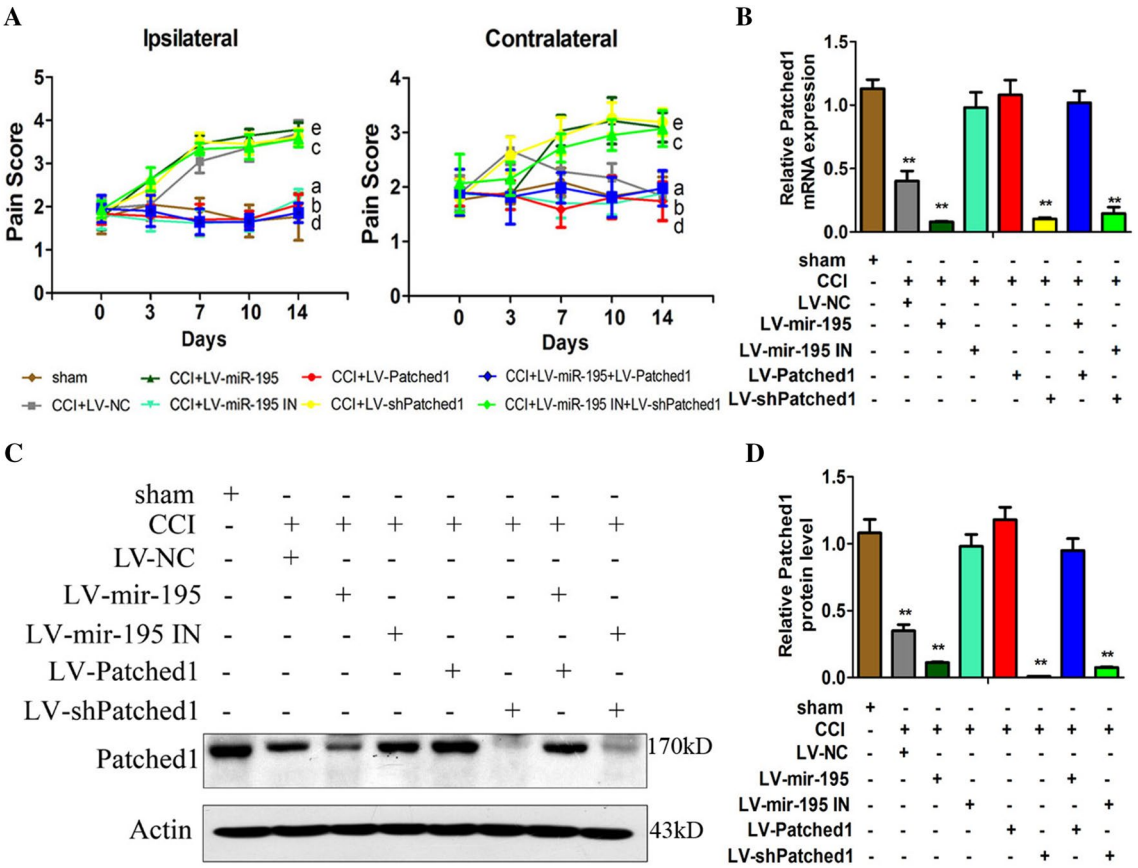

Fig. 5 Patched1 is Responsible for miR-195-mediated Neuropathic Pain. **a** The effect on neuropathic pain was assessed by behavioral testing and analysis on days 0, 3, 7, 10 and 14 by infecting rats with LV-miR-195, LV-miR-195 inhibitor, LV-Patched1, or LV-sh Patched1, or coinfecting the rats with LV-miR-195 and LV-Patched1 or LV-miR-195 inhibitor and LV-sh Patched1 after CCI-IoN. [a]$p<0.01$ (CCI + LV-miR-195 inhibitor vs. CCI + LV-miR-195); [b]$p<0.01$ (CCI + LV-Patched1 vs. CCI + LV − NC); [c]$p<0.01$ (CCI + LV-sh Patched1 vs. CCI + LV-Patched1); [d]$p<0.01$ (CCI + LV-miR-195 + LV-Patched1 vs. CCI + LV-miR-195); [e]$p<0.01$ (CCI + LV-miR-195 inhibitor + LV-sh Patched1 vs. CCI + LV-miR-195 inhibitor). **b** The relative expression of Patched1 mRNA and protein **c**, **d** was detected by RT-PCR and Western blotting on day 7. $^{**}p<0.01$ versus sham group. N = 6 for each group in a and b. N = 3 for each group in **c** and **d**

or astrocytes. In addition, they demonstrated upregulated expression of miR-195 in isolated primary microglial cells. The regulation and expression patterns of miRNAs were always varied according to temporal-spatial specificity and stimulus-dependence [22, 23]; this method likely affected the accuracy of the results.

miR-195 is a member of the miR-15/107 family, is only expressed in mammals, and is expressed especially in the central nervous system [24]. Rapid upregulated and long-term expression is observed after peripheral nerve ligation [25]. Existing evidence shows that miR-195 is mainly involved in neuroprotection against some neural injuries and alleviates dementia induced by chronic brain hypoperfusion and Alzheimer's disease via multiple targets [26, 27], including BDNF and VAMP1, which have been verified by many studies to play pivotal roles in neuropathic pain [28]. In addition, miR-195 contributes to the differentiation of neural stem cells and nerve regeneration [29], and these processes were generally observed to participate in neuropathic pain. Many noncoding RNAs, especially microRNAs, including miR-183, 195, 124, and 125, have been shown to play key roles in pain caused by peripheral nerve injury and inflammation [3, 4]. As an example, Aldrich et al. found that, in animals that underwent spinal nerve ligation (SNL), the expression of the miR-183 family significantly decreased [30], and an intrathecal injection of miR-183 suppressed mechanical allodynia in rats with neuropathic pain [31]. Recently, more advanced studies demonstrated that miR-183 targets the auxiliary voltage-gated calcium channel subunits α2δ-1 and α2δ-2 and a special, light-touch-sensitive neuronal type that normally does not elicit pain but is recruited during mechanical allodynia [5]. In these ways, miR-183, a single microRNA cluster, can continuously control acute noxious mechanical sensitivity in nociceptive neurons and suppress neuropathic pain transduction.

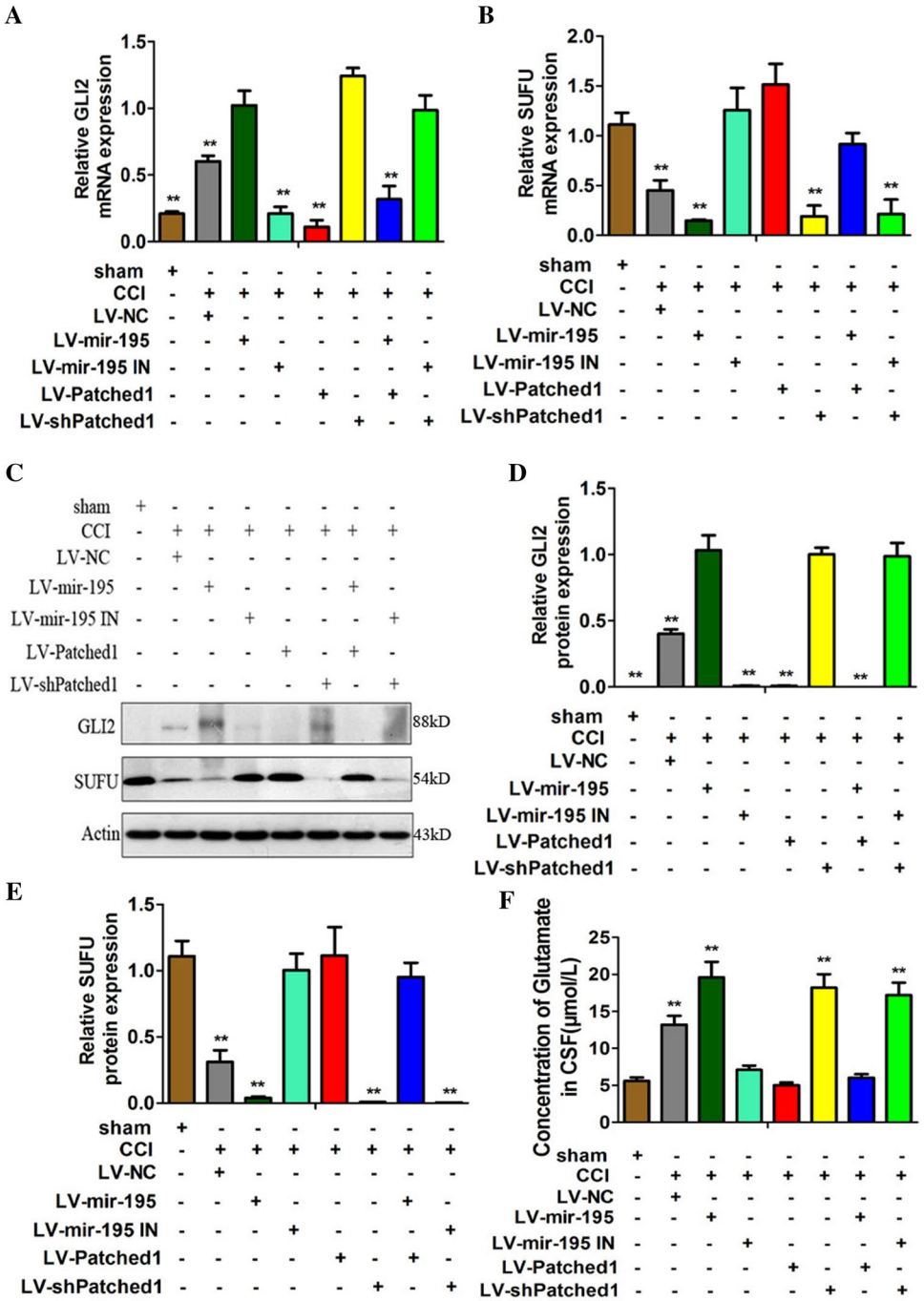

Fig. 6 miR-195 increases the extracellular glutamate levels and is Involved in TN Through the SHH Signaling Pathway. The Gli2 mRNA and protein (**a, c** and **d**) expression levels were measured by RT-PCR and Western blotting on day 7. $^{**}p < 0.01$ versus CCI + LV-miR-195. **b** The SUFU mRNA and protein (**b, c** and **e**) expression levels were measured by RT-PCR and Western blotting on day 7. $^{**}p < 0.01$ versus sham group. **f** The concentration of glutamate was measured in the cerebrospinal fluid (CSF) of the rat model on day 7. $^{**}p < 0.01$ versus sham. N = 6 for each group in **a**, **b** and **f**. N = 3 for each group in **c**, **d** and **e**

In this study, using Target Scan software, the seed sequence of miR-195 was paired with the Patched1 3′-UTR in both humans and rats. By using a luciferase assay, we verified that miR-195 negatively regulates Patched1 by binding to with the Patched1 3′-UTR. As expected, the transfection of scrambled miRNA or mutant Patched1 3′-UTR was not able to significantly change the firefly/Renilla ratio, indicating that miR-195 and the 3′-UTR of Patched1 are specific. Moreover, Patched1 mRNA and protein expression levels were inhibited in a dose-dependent manner by the transfection of miR-195 mimics. Consistent with the results obtained in 293T cells, Patched1 was increased at both the mRNA and protein levels upon intracerebroventricular injection of LV-miR-195, which was significantly increased by intracerebroventricular injection of LV-miR-195 inhibitor in the caudal medulla of TN rats. In addition, we demonstrated that miR-195 aggravated pain by inhibiting Patched1 through the evaluation of behavior and changes in molecular levels in TN rats. Moreover, we also found that an intracerebroventricular injection of LV-miR-195 inhibitor contributed

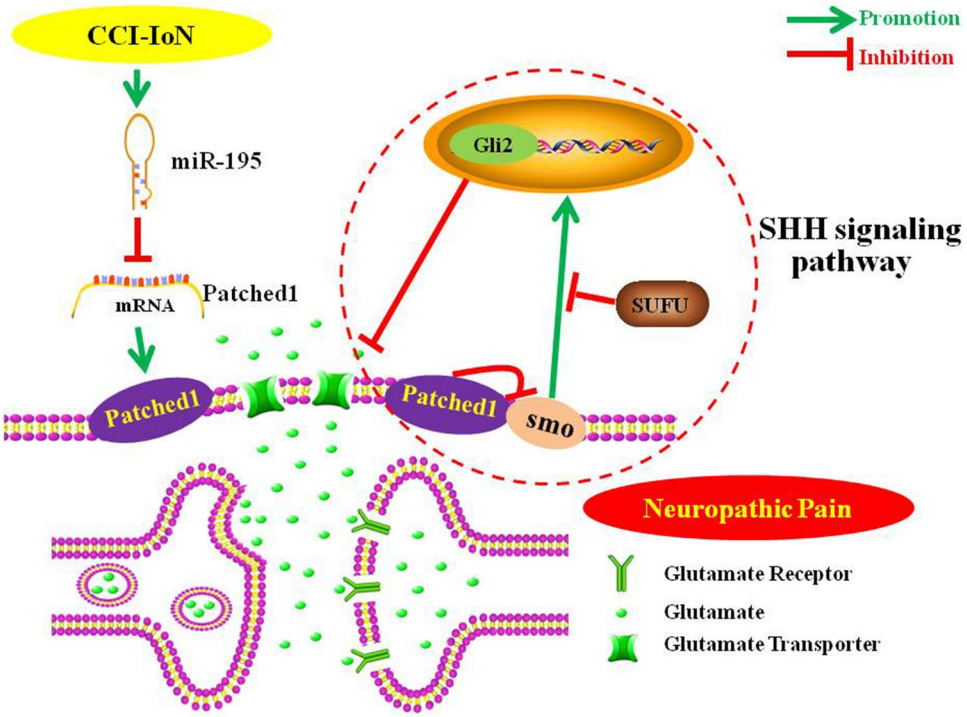

Fig. 7 A schematic diagram showing that miR-195 aggravates mechanical allodynia in CCI rats by upregulating the Shh signaling pathway. miR-195 is upregulated due to the CCI-IoN procedure, and it targets Patched1, an inhibitory receptor of Shh signal, and reduces its expression, resulting in the activation of the Shh signaling pathway (and regulating its downstream factors Gli2 and SUFU). The activation of the Shh signaling pathway aggravates facial pain by elevating the concentration of extracellular glutamate

to the alleviation of pain behaviors and the upregulation of Patched1 in the caudal medulla of TN rats. This evidence reveals that miR-195 and Patched1 are crucial players in neuropathic pain, implying that miR-195 inhibitors and Patched1 might be practical drug targets for the treatment of TN.

Our results showed that the mRNA and protein expression levels of Patched1 were significantly decreased in the caudal medulla of the TN group compared with the sham group, suggesting that Patched1 levels are inversely related to the levels of miR-195. In vivo, in contrast to the results obtained upon infection with LV-miR-195 and LV-miR-195 inhibitor, the administration of LV-Patched1 significantly decreased facial pain, and LV-sh Patched1 lessened facial pain, which was still observed easily on the contralateral side. Existing studies have shown that the Shh signaling pathway may be involved in neuropathic pain by increasing the permeability of the blood–nerve barrier and enhancing neuroinflammation [13]. Additionally, Shh signaling participates in epilepsy development by inhibiting glutamate transporters, resulting in an elevated level of extracellular glutamate [20], which is an important factor related to neuropathic pain [19, 21]. Here, we tested the glutamate concentration in the cerebrospinal fluid (CSF) and found that the glutamate levels in the CSF were markedly increased in the CCI-IoN group compared with the sham group, were increased by LV-miR-195 infection, and were markedly decreased by infection with the miR-195 inhibitor. The administration of LV-Patched1 and LV-sh Patched1 decreased and increased the glutamate levels in the CSF, respectively, and influenced facial pain. These results suggest that Shh is involved in TN by regulating extracellular glutamate levels. Previous studies have shown that Shh signaling plays an important role in the development and patterning of the central nervous system and other organs [8] and influences the development of some peripheral nerves, including the trigeminal nerve, facial nerve [32], and spinal nerve [33] and the sympathetic nervous system [34]. All Shh pathway components can be found in the mature brain [35], but their functions are not completely clear. Recent evidence has shown that Shh may be secreted by dying cells and induce compensatory proliferation and remyelination after tissue injury [10, 11], which stimulates mature astrocytes during nerve injury and results in reactive gliosis and inflammation [36]. These can be seen in TN patients and CCI-IoN animal models [37, 38]. Furthermore, Shh family molecules are expressed in many structures involved in the pain pathway. Martinez et al. suggested that essential members of the Shh signaling pathway, including the Shh protein, Patched1, SMO, Gli2 and Gli3, are expressed in adult dorsal root ganglia (DRG) and upregulated following sciatic injury; this expression pattern facilitates the regeneration of axons and Schwann cells [39]. However, only a few studies have focused on the relationship between the Shh pathway and neuropathic pain. One study demonstrated that Shh signaling is required for thermal allodynia and hyperalgesia. Intrathecal or peripheral administration of a special inhibitor of SMO suppresses inflammatory pain and enhances and sustains morphine analgia in animals

with neuropathic pain [12]. Another study showed that Shh signaling in vascular endothelial cells participates in neuropathic pain development by disrupting the blood-nerve barrier and inducing local inflammation [13].

There are some limitations to our study. Our animal model of CCI-IoN did not simulate typical TN or orofacial neuropathic pain well. Although several other TN animal models, including a model involving the ligation of the infraorbital nerve and the facial tissue inflammation model [40], have been developed, all the models face this limitation. It is well known that a single microRNA has many targets. However, including our results, there are only two known mechanisms by which miR-195 influences neuropathic pain. Therefore, we have no way to evaluate the weight of our results on the field. Although there was no significant change in miR-195 expression in neurons after the surgeries, we should not ignore this process. We will investigate the underlying role of miR-195 in neurons in subsequent studies.

Acknowledgments This work was supported by the National Natural Science Foundation of China (Grants Nos. 81300965, 81402513 and 81472596), the Outstanding Researcher Fund of Third Military Medical University (Army Medical University) (No. 2017MPRC-17), and the Intramural project by Southwestern Hospital (SWH2016LHJC-06). MX and SC conceived the project, supervised all experiments, and wrote the manuscript. XW designed the project, collected the data, and wrote the manuscript. LX supervised the experiments and analyzed the data. Hong W and Hao W researched the data and conducted behavioral tests. All authors read and approved the final manuscript.

Compliance with Ethical Standards

Conflict of interest The authors declare no conflicts of interest.

References

1. Velagala J, Mendelson ZS, Liu JK (2015) 186Pain-free outcomes after surgical intervention for trigeminal neuralgia: a comparison of gamma knife and microvascular decompression. Neurosurgery 62(Suppl):1
2. Benarroch EE (2010) Central neuron-glia interactions and neuropathic pain: overview of recent concepts and clinical implications. Neurology 75:273–278
3. Lutz BM, Bekker A, Tao YX (2014) Noncoding RNAs: new players in chronic pain. Anesthesiology 121:409–417
4. McDonald MK, Ajit SK (2015) MicroRNA biology and pain. Progr Mol Biol Transl Sci 131:215–249
5. Peng C, Li L, Zhang MD, Bengtsson Gonzales C, Parisien M, Belfer I, Usoskin D, Abdo H, Furlan A, Haring M, Lallemend F, Harkany T, Diatchenko L, Hokfelt T, Hjerling-Leffler J, Ernfors P (2017) miR-183 cluster scales mechanical pain sensitivity by regulating basal and neuropathic pain genes. Science 356:1168–1171
6. Shi G, Shi J, Liu K, Liu N, Wang Y, Fu Z, Ding J, Jia L, Yuan W (2013) Increased miR-195 aggravates neuropathic pain by inhibiting autophagy following peripheral nerve injury. Glia 61:504–512
7. Briscoe J, Therond PP (2013) The mechanisms of Hedgehog signalling and its roles in development and disease. Nat Rev Mol Cell Biol 14:416–429
8. Ruiz i Altaba A, Palma V, Dahmane N (2002) Hedgehog-Gli signalling and the growth of the brain. Nat Rev Neurosci 3:24–33
9. Robbins DJ, Fei DL, Riobo NA (2012) The Hedgehog signal transduction network. Sci Signal 5:re6
10. Fan Y, Bergmann A (2008) Distinct mechanisms of apoptosis-induced compensatory proliferation in proliferating and differentiating tissues in the Drosophila eye. Dev Cell 14:399–410
11. Perez-Garijo A, Shlevkov E, Morata G (2009) The role of Dpp and Wg in compensatory proliferation and in the formation of hyperplastic overgrowths caused by apoptotic cells in the Drosophila wing disc. Development 136:1169–1177
12. Babcock DT, Shi S, Jo J, Shaw M, Gutstein HB, Galko MJ (2011) Hedgehog signaling regulates nociceptive sensitization. Curr Biol 21:1525–1533
13. Moreau N, Mauborgne A, Bourgoin S, Couraud PO, Romero IA, Weksler BB, Villanueva L, Pohl M, Boucher Y (2016) Early alterations of Hedgehog signaling pathway in vascular endothelial cells after peripheral nerve injury elicit blood-nerve barrier disruption, nerve inflammation, and neuropathic pain development. Pain 157:827–839
14. Vos BP, Strassman AM, Maciewicz RJ (1994) Behavioral evidence of trigeminal neuropathic pain following chronic constriction injury to the rat's infraorbital nerve. J Neurosci 14:2708–2723
15. Dieb W, Hafidi A (2013) Astrocytes are involved in trigeminal dynamic mechanical allodynia: potential role of D-serine. J Dent Res 92:808–813
16. Han M, Xiao X, Yang Y, Huang RY, Cao H, Zhao ZQ, Zhang YQ (2014) SIP30 is required for neuropathic pain-evoked aversion in rats. J Neurosci 34:346–355
17. Paxinos G, Watson C (2007) The rat brain in stereotaxic coordinates, 6th edn. Academic Press, Sydney
18. Hara K, Haranishi Y, Terada T, Takahashi Y, Nakamura M, Sata T (2014) Effects of intrathecal and intracerebroventricular administration of luteolin in a rat neuropathic pain model. Pharmacol Biochem Behav 125:78–84
19. Inquimbert P, Bartels K, Babaniyi OB, Barrett LB, Tegeder I, Scholz J (2012) Peripheral nerve injury produces a sustained shift in the balance between glutamate release and uptake in the dorsal horn of the spinal cord. Pain 153:2422–2431
20. Feng S, Ma S, Jia C, Su Y, Yang S, Zhou K, Liu Y, Cheng J, Lu D, Fan L, Wang Y (2016) Sonic hedgehog is a regulator of extracellular glutamate levels and epilepsy. EMBO Rep 17:682–694
21. Liaw WJ, Stephens RL Jr, Binns BC, Chu Y, Sepkuty JP, Johns RA, Rothstein JD, Tao YX (2005) Spinal glutamate uptake is critical for maintaining normal sensory transmission in rat spinal cord. Pain 115:60–70
22. Bai G, Ambalavanar R, Wei D, Dessem D (2007) Downregulation of selective microRNAs in trigeminal ganglion neurons following inflammatory muscle pain. Mol Pain 3:15
23. Kusuda R, Cadetti F, Ravanelli MI, Sousa TA, Zanon S, De Lucca FL, Lucas G (2011) Differential expression of microRNAs in mouse pain models. Mol Pain 7:17
24. Wang WX, Danaher RJ, Miller CS, Berger JR, Nubia VG, Wilfred BS, Neltner JH, Norris CM, Nelson PT (2014) Expression of miR-15/107 family microRNAs in human tissues and cultured rat brain cells. Genom Proteom Bioinform 12:19–30
25. Yu B, Zhou S, Wang Y, Ding G, Ding F, Gu X (2011) Profile of microRNAs following rat sciatic nerve injury by deep sequencing: implication for mechanisms of nerve regeneration. PLoS ONE 6:e24612
26. Sun LH, Ban T, Liu CD, Chen QX, Wang X, Yan ML, Hu XL, Su XL, Bao YN, Sun LL, Zhao LJ, Pei SC, Jiang XM, Zong DK, Ai J (2015) Activation of Cdk5/p25 and tau phosphorylation following chronic brain hypoperfusion in rats involves microRNA-195 down-regulation. J Neurochem 134:1139–1151

27. Zhu HC, Wang LM, Wang M, Song B, Tan S, Teng JF, Duan DX (2012) MicroRNA-195 downregulates Alzheimer's disease amyloid-beta production by targeting BACE1. Brain Res Bull 88:596–601
28. Finnerty JR, Wang WX, Hebert SS, Wilfred BR, Mao G, Nelson PT (2010) The miR-15/107 group of microRNA genes: evolutionary biology, cellular functions, and roles in human diseases. J Mol Biol 402:491–509
29. Liu C, Teng ZQ, McQuate AL, Jobe EM, Christ CC, von Hoyningen-Huene SJ, Reyes MD, Polich ED, Xing Y, Li Y, Guo W, Zhao X (2013) An epigenetic feedback regulatory loop involving microRNA-195 and MBD1 governs neural stem cell differentiation. PLoS ONE 8:e51436
30. Aldrich BT, Frakes EP, Kasuya J, Hammond DL, Kitamoto T (2009) Changes in expression of sensory organ-specific microRNAs in rat dorsal root ganglia in association with mechanical hypersensitivity induced by spinal nerve ligation. Neuroscience 164:711–723
31. Lin CR, Chen KH, Yang CH, Huang HW, Sheen-Chen SM (2014) Intrathecal miR-183 delivery suppresses mechanical allodynia in mononeuropathic rats. Eur J Neurosci 39:1682–1689
32. Kurosaka H, Trainor PA, Leroux-Berger M, Iulianella A (2015) Cranial nerve development requires co-ordinated Shh and canonical Wnt signaling. PLoS ONE 10:e0120821
33. Guan W, Wang G, Scott SA, Condic ML (2008) Shh influences cell number and the distribution of neuronal subtypes in dorsal root ganglia. Dev Biol 314:317–328
34. Morikawa Y, Maska E, Brody H, Cserjesi P (2009) Sonic hedgehog signaling is required for sympathetic nervous system development. NeuroReport 20:684–688
35. Traiffort E, Charytoniuk D, Watroba L, Faure H, Sales N, Ruat M (1999) Discrete localizations of hedgehog signalling components in the developing and adult rat nervous system. Eur J Neurosci 11:3199–3214
36. Alvarez-Buylla A, Ihrie RA (2014) Sonic hedgehog signaling in the postnatal brain. Semin Cell Dev Biol 33:105–111
37. Love S, Coakham HB (2001) Trigeminal neuralgia: pathology and pathogenesis. Brain 124:2347–2360
38. Xu M, Aita M, Chavkin C (2008) Partial infraorbital nerve ligation as a model of trigeminal nerve injury in the mouse: behavioral, neural, and glial reactions. J Pain 9:1036–1048
39. Martinez JA, Kobayashi M, Krishnan A, Webber C, Christie K, Guo G, Singh V, Zochodne DW (2015) Intrinsic facilitation of adult peripheral nerve regeneration by the Sonic hedgehog morphogen. Exp Neurol 271:493–505
40. Yeomans DC, Klukinov M (2012) A rodent model of trigeminal neuralgia. Methods Mol Biol 851:121–131